J. Condensed Matter Nucl. Sci. 9 (2012) 30–49

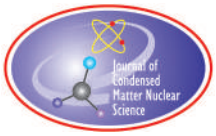


Research Article

# Pulse and Amplitude Approximation for the Lossy Spin–Boson Model

Peter L. Hagelstein *

*Research Laboratory of Electronics, Massachusetts Institute of Technology, Cambridge, MA 02139, USA*

Irfan U. Chaudhary

*Department of Computer Science and Engineering, University of Engineering and Technology. Lahore, Pakistan*

**Abstract**

The lossy spin-boson model is of interest to us since it predicts efficient energy exchange between identical two-level systems and an oscillator when the transition energy is a large (odd) multiple of the the oscillator energy. This model is not so easy to solve directly in the strong coupling regime, so we have developed approximate versions of the model that are easier to analyze. Here we introduce the pulse and amplitude approximation which compares very well with exact numerical solutions when the coupling is strong, and when the characteristic oscillator energy is much less than the transition energy. We examine discrete and continuum versions of the approximation, and find that they give good results for the solutions and for the self-energy. We show that the indirect coupling matrix element can be estimated from differences in the eigenvalue of the pulse optimization constraint for solutions with different phases.
 ISSN 2227-3123

*Keywords:* Fleischmann–Pons effect, Lossy spin–boson model, Phonon exchange, Quantum fractionation

## 1. Introduction

In previous publications we introduced the lossy spin–boson model [1–5], which has the interesting property that it describes efficient coherent energy exchange between a set of identical two-level systems and and oscillator under conditions where the transition energy of the two-level systems is very much greater than the oscillator energy. The fractionation of a large quantum into a great many small quanta constitutes a new physical effect that may have applications in different fields, and for this reason alone merits further study. Our motivation for pursuing the model comes from trying to understand excess heat production in the Fleischmann–Pons experiment [6,7].

*E-mail: plh@mit.edu

 ISSN 2227-3123

The model predicts that the dimensionless coupling constant $g$ must be large in order to fractionate a two-level quantum into more oscillator quanta. The associated scaling parameter for this process in the model is $g/\Delta n^2$, where $\Delta n$ is the number of oscillator quanta that make up the transition energy $\Delta E$

$$\Delta E \;=\; \Delta n \hbar \omega_0, \tag{1}$$

where $\hbar\omega_0$ is the characteristic oscillator energy. To fractionate a large quantum into ten times as many oscillator quanta requires a dimensionless coupling constant larger by one hundred. We view this scaling as relatively gentle, suggesting that in a physical system for which the model applies, it should be "easy" to fractionate the two-level system quantum.

In the analysis reported previously, we developed a simplified version of the model that we were able to solve using a combination of numerical and analytical methods. In this work we examine the approximate solution for the eigenfunctions and eigenvalues using a separable eigenfunction; the ideas behind this approach were described briefly previously [5]. Our goal here is to provide a more systematic version of the approximation. This analysis is useful for the lossy spin–boson model with infinite loss, and perhaps more importantly lays the foundation for a systematic approximation that we can use for more complicated models based on three and more levels in place of the two-level system model.

## 2. Basic Model

The sector Hamiltonian for the lossy spin–boson model is [1]

$$\hat{H} \;=\; \frac{\Delta E}{\hbar}\hat{S}_z + \hbar\omega_0 \hat{a}^\dagger \hat{a} + V(\hat{a}^\dagger + \hat{a})\frac{2\hat{S}_x}{\hbar} - i\frac{\hbar\hat{\Gamma}(E)}{2}. \tag{2}$$

This model in general is very difficult to solve, especially in the strong coupling limit which is of interest to us since we would like to study coherent energy exchange under conditions where the large quantum of the two-level system is fractionated. A great simplification comes about in perturbation theory calculations if we assume that the loss is infinitely large for basis states with energies less than $E$; such states are removed from the problem with this assumption since their occupation probability becomes vanishingly small as the loss goes to infinity.

### 2.1. Local approximation

We are interested in the eigenfunctions and eigenvalues of the Schrödinger equation

$$E\Psi \;=\; \hat{H}\Psi. \tag{3}$$

If we use a basis expansion of the form

$$\Psi \;=\; \sum_m \sum_n c_{m,n} |S, m\rangle |n\rangle, \tag{4}$$

then the expansion coefficients $c_{m,n}$ satisfy

$$Ec_{m,n} \;=\; \left(\Delta E m + \hbar\omega_0 n - i\frac{\hbar}{2}\Gamma(E)\right)c_{m,n} + V\sqrt{n+1}\sqrt{(S-m)(S+m-1)}c_{m+1,n+1}$$

$$+V\sqrt{n}\sqrt{(S-m)(S+m-1)}c_{m+1,n-1}+V\sqrt{n+1}\sqrt{(S+m)(S-m+1)}c_{m-1,n+1}$$

$$+V\sqrt{n}\sqrt{(S+m)(S-m+1)}c_{m-1,n-1}. \tag{5}$$

In the limit of large $n$ and large $\sqrt{S^2-m^2}$, the different factors of the interaction terms become nearly the same, which suggests that we might make progress by studying a version of the problem in which the coefficients are all the same. This problem can be written as

$$Ec_{m,n} = \left[\Delta Em+\hbar\omega_0 n - i\frac{\hbar}{2}\Gamma(E)\right]c_{m,n}$$

$$+V\sqrt{n}\sqrt{S^2-m^2}\Big(c_{m+1,n+1}+c_{m+1,n-1}+c_{m-1,n+1}+c_{m-1,n-1}\Big). \tag{6}$$

We term this the local approximation [4].

## 2.2. Periodic model

If we assume that the system is in resonance

$$\Delta E = \Delta n\hbar\omega_0 \tag{7}$$

with integer $\Delta n$, then the model becomes periodic under energy conserving translations. This allows us to make use of Bloch's theorem, which has the practical consequence of reducing a two-dimensional calculation to a set of calculations in one dimension. We can implement Bloch's theorem by adopting a solution of the form

$$\Psi = \sum_m \sum_n \mathrm{e}^{im\phi} v_{n+m\Delta n}|S,m\rangle|n\rangle. \tag{8}$$

The $v$ expansion coefficients satisfy [4]

$$E(\phi)v_n = \left[n\hbar\omega_0 - i\frac{\hbar}{2}\hat{\Gamma}(E)\right]v_n$$

$$+g\Delta E\Big[\mathrm{e}^{i\phi}(v_{n+\Delta n+1}+v_{n+\Delta n-1})+\mathrm{e}^{-i\phi}(v_{n-\Delta n+1}+v_{n-\Delta n-1})\Big], \tag{9}$$

where the dimensionless coupling constant $g$ is defined as

$$g = \frac{V\sqrt{n}\sqrt{S^2-m^2}}{\Delta E}. \tag{10}$$

### 2.3. Implementing loss as a hard boundary

In the limit of infinite loss, we eliminated the basis states in perturbation theory with an energy less than $E$. In the strong coupling limit, the self-energy is sufficiently large that it becomes difficult to implement such a scheme. It ends up being simpler to eliminate basis states below a fixed basis state energy, which we can implement here by adopting a hard boundary in $n$. It is convenient in this limit to work with a relative $n$ that is zero just above the boundary. This leads to an eigenvalue equation of the form [5]

$$E(\phi)v_n \;=\; n\hbar\omega_0 + g\Delta E\left[e^{i\phi}(v_{n+\Delta n+1} + v_{n+\Delta n-1}) + e^{-i\phi}(v_{n-\Delta n+1} + v_{n-\Delta n-1})\right] \tag{11}$$

with the condition

$$v_n \;=\; 0 \qquad \text{for } n < 0. \tag{12}$$

### 2.4. Indirect coupling coefficients and system dynamics

The system dynamics can be approximated using a model based on indirect coupling between sequential nearly degenerate states. For coherent energy exchange when $\Delta n$ is large, the associated rate is determined by the indirect coupling coefficient between states that differ according to

$$(m, n) \;\rightarrow\; (m \pm 1, n \mp \Delta n). \tag{13}$$

Since the indirect coupling is strongest between these states, we can estimate the indirect coupling matrix element $V_{eff}$ from the level splitting [3]

$$V_{\text{eff}} \;=\; \frac{E(0) - E(\pi)}{4}. \tag{14}$$

The system dynamics developed from Ehrenfest's theorem for the classical average $m(t)$ when the states are degenerate satisfy [2]

$$\frac{d^2}{dt^2}m(t) \;=\; \frac{2}{\hbar^2}\frac{d}{dm}.V_{\text{eff}}^2(m). \tag{15}$$

Consequently, our primary focus is on the determination of the indirect coupling matrix elements $V_{\text{eff}}$ in what follows.

## 3. Pulse and Envelope Approximation

Even though the various approximations we have introduced simplify the problem considerably, the eigenvalue equation for the $v_n$ expansion coefficients can still be difficult to solve when the coupling is strong. We are interested in developing an approximate product solution that will model the shape of individual "pulses" separately from the "envelope".

### 3.1. Energy

Although we obtained approximate equations previously for the pulse shape and amplitude, here we would like to be more systematic. The starting point for our analysis is total energy, which we write as

$$\langle v_n|\hat{H}|v_n\rangle \;=\; \hbar\omega_0 \sum_n n|v_n|^2$$

$$+g\Delta E \sum v_n^* \Big[ \mathrm{e}^{i\phi}(v_{n+\Delta n+1} + v_{n+\Delta n-1}) + \mathrm{e}^{-i\phi}(v_{n-\Delta n+1} + v_{n-\Delta n-1}) \Big]. \tag{16}$$

Ideally, we would like to implement our approximation to derive a new energy relation in terms of a pulse shape and amplitudes, and then minimize the energy to obtain variational equations for the pulse and amplitudes.

### 3.2. Approximate product solutions for $\phi = 0$ and $\phi = \pi$

We adopt approximate product solutions given by (see the solutions for the expansion coefficients in [5])

$$v_n \;=\; \sum_m (-1)^m a_m u_{n-m\Delta n} \qquad (\phi = 0), \tag{17}$$

$$v_n \;=\; \sum_m a_m u_{n-m\Delta n} \qquad (\phi = \pi). \tag{18}$$

The idea is that a single pulse is modeled using the $u_n$ within a range of $\Delta n$ indices, and successive pulses are scaled with the amplitude $a_m$ (where the $m$ index keeps track of the pulse). We include the phase factor for the $\phi = 0$ case since successive pulses are observed to alternate in sign in numerical calculations.

The energy expression in both cases is the same algebraically; we may write

$$\langle v_n|\hat{H}|v_n\rangle \;=\; \Delta E \sum_m m a_m^2 \;+\; \hbar\omega_0 \sum_n n u_n^2$$

$$-g\Delta E \sum_m a_m(a_{m+1} + a_{m-1}) \sum_n u_n(u_{n+1} + u_{n-1}), \tag{19}$$

where we have assumed that

$$\sum_n u_n^2 \;=\; 1, \qquad \sum_m a_m^2 \;=\; 1. \tag{20}$$

### 3.3. Optimization of the pulse and envelope

We can optimize the pulse shape $u_n$ by minimizing the energy subject to the constraint that the associated probability is constant to obtain

$$\lambda_u u_n \;=\; \frac{n}{\Delta n} u_n - g\Big[ \sum_m a_m(a_{m+1} + a_{m-1}) \Big](u_{n+1} + u_{n-1}). \tag{21}$$

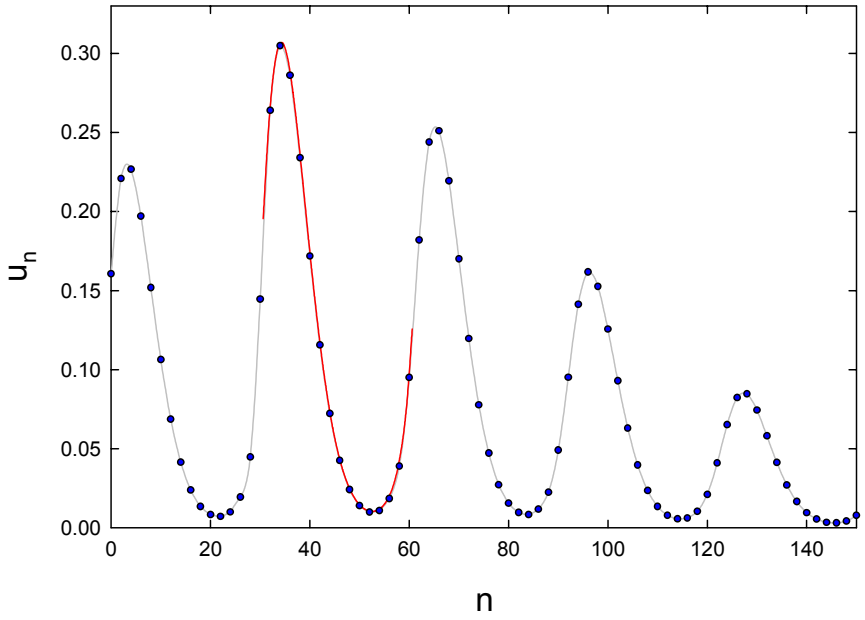


**Figure 1.** Expansion coefficients for $\Delta n = 31$, $g = 2$, and $\phi = \pi$ (*blue points*); optimized product solution for the pulse (*red line*).

The boundary conditions for the $u_n$ for the two cases within this approximation are

$$u_n = -u_{n+\Delta n} \quad (\phi = 0), \tag{22}$$

$$u_n = u_{n+\Delta n} \quad (\phi = \pi). \tag{23}$$

A similar argument can be used to optimize the envelope $a_m$ to obtain

$$\lambda_a a_m = m a_m - g\left[\sum_n u_n (u_{n+1} + u_{n-1})\right](a_{m+1} + a_{m-1}). \tag{24}$$

The boundary conditions appropriate are

$$a_{-m} = 0 \quad (m = 1, 2, \cdots), \tag{25}$$

$$\lim_{m\to\infty} a_m = 0. \tag{26}$$

### 3.4. Evaluation of the discrete pulse and envelope model

The formulation that we have outlined above allows us to optimize pulse shapes and amplitudes systematically, and provides a route for the computation of the total energy. In principle, all we need to do is to carry out such computations in order to develop approximate results for the energy splitting needed to estimate the indirect coupling. The approach works pretty well, as we can see from comparing with a test problem.

Consider the specific example of $\Delta n = 31$ and $g = 2$. We can see how good the approximate pulse solution is by comparing it to a numerically exact solution in Fig. 1. The optimized approximate pulse shape compares well with the exact solution. The optimized amplitudes are shown in comparison with the exact solution for the expansion coefficients in Fig. 2, where one sees again that the agreement is good.

The total energies for the numerically exact solution are

$$E(0) = -5.0856160\ \Delta E, \qquad E(\pi) = -5.0859317\ \Delta E. \tag{27}$$

The total energies for the approximate solution are evaluated from the total energy expression of Eq. (19)

$$E(0) = -5.0723289\ \Delta E, \qquad E(\pi) = -5.0726649\ \Delta E. \tag{28}$$

The approximate self-energies are reasonably close to the numerically exact results (see Fig. 3). The indirect coupling matrix element in the numerically exact calculation is

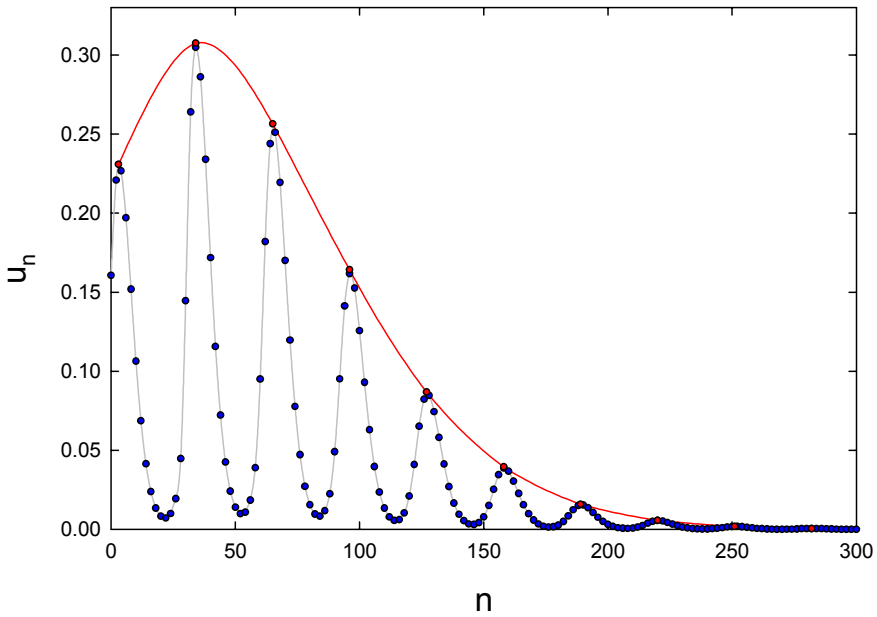


**Figure 2.** Expansion coefficients for $\Delta n = 31$, $g = 2$, and $\phi = \pi$ (*blue points*); optimized product solution for the amplitude (*red points*).

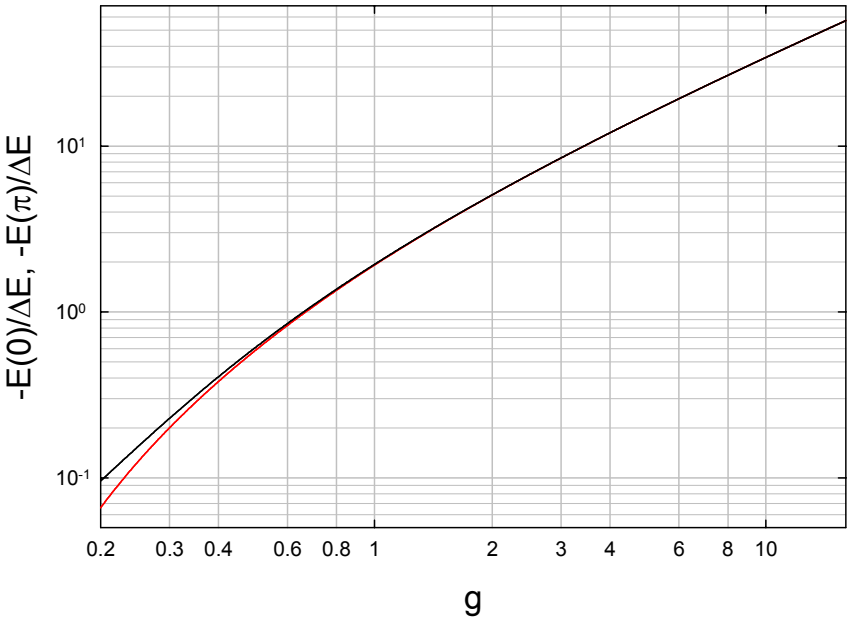


**Figure 3.** Self-energy as a function of $g$ for $\Delta n = 31$; numerically exact results (*black*), and results computed from optimized pulse and amplitudes (*red*).

$$\frac{V_{\rm eff}}{\Delta E} = 7.89137 \times 10^{-5}. \tag{29}$$

For the approximation, we get

$$\frac{V_{\rm eff}}{\Delta E} = 8.40067 \times 10^{-5}, \tag{30}$$

which from our perspective is reasonable, since this quantity changes rapidly with $g$ as can be seen in Fig. 4. The approximate indirect coupling matrix element begins to diverge from the exact result at small $g$, which might be expected as the solution in this regime is dominated by a single narrow pulse.

Our basic conclusion is that the pulse and amplitude approximation works pretty well for this problem.

## 4. Continuum Pulse and Discrete Envelope Approximation

We are interested in lossy spin–boson models and their generalizations under conditions where $\Delta n$ is very large, in which case we would like to use a continuum approximation for the pulse. For now, we will keep the envelope discrete as in the model of the previous section.

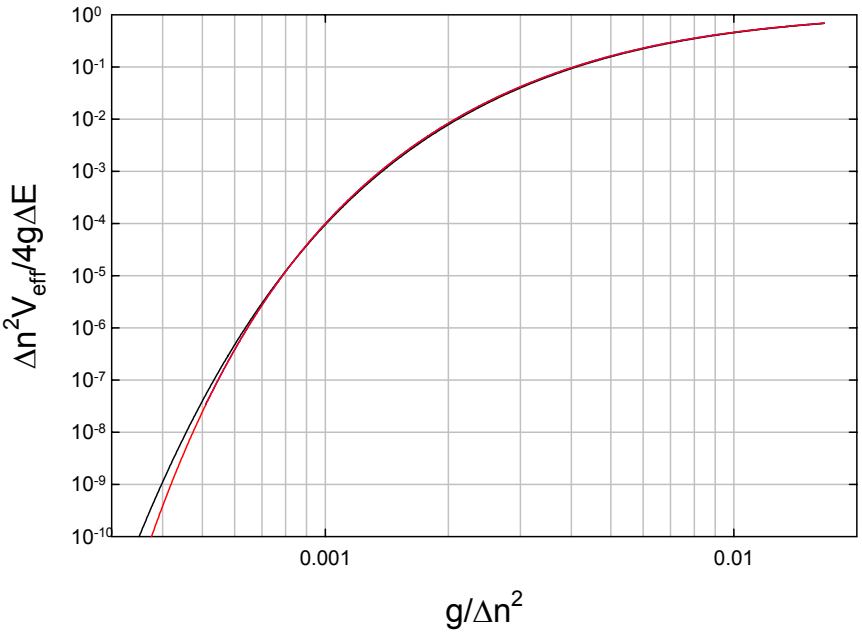


**Figure 4.** Scaled indirect coupling matrix element as a function of $g$ for $\Delta n = 31$; numerically exact result (*black*), and scaled matrix element computed from optimized discrete pulse and amplitudes (*red*).

### 4.1. Pulse continuum approximation

We begin by defining a continuum variable associated with the $n$ index

$$\frac{n}{\Delta n} \;\rightarrow\; z \tag{31}$$

and then allow the pulse to be a continuous functions

$$u_n \;\rightarrow\; u(z). \tag{32}$$

The energy expression with a continuous pulse can be written as

$$\langle v_n|\hat{H}|v_n\rangle \;=\; \Delta E \sum_m m a_m^2 \;+\; \Delta E \int_0^1 z u^2(z)\,\mathrm{d}z$$

$$-g\Delta E \sum_m a_m (a_{m+1} + a_{m-1}) \int_0^1 u(z) \left[ u\left(z + \frac{1}{\Delta n}\right) + u\left(z - \frac{1}{\Delta n}\right)\right] \mathrm{d}z, \tag{33}$$

where we assume that

$$\sum_m a_m^2 \;=\; 1, \tag{34}$$

$$\int_0^1 u^2(z)\,\mathrm{d}z \;=\; 1. \tag{35}$$

4.2. Large $\Delta n$ limit

Although it is possible to develop a continuum model based on the energy expression above, the resulting optimization of the pulse will involve a difference-differential eigenvalue constraint that is not particularly easy to solve. We would prefer a differential eigenvalue equation. The continuum approximation would be used for problems where many indices $n$ are involved, which occurs when $\Delta n$ is large. So, it seems reasonable to assume that $\Delta n$ will be large, and we may approximate

$$u\left(z+\frac{1}{\Delta n}\right)+u\left(z-\frac{1}{\Delta n}\right) \;=\; 2u(z)+\frac{1}{\Delta n^2}\frac{\mathrm{d}^2}{\mathrm{d}z^2}u(z)+\cdots \tag{36}$$

If a second order approximation is sufficient, then the integral in the energy expression can be recast as

$$\begin{aligned}\int_0^1 u(z)\left[u\left(z+\frac{1}{\Delta n}\right)+u\left(z-\frac{1}{\Delta n}\right)\right]\mathrm{d}z \;&=\; \int_0^1 u(z)\left[2u(z)+\frac{1}{\Delta n^2}\frac{\mathrm{d}^2}{\mathrm{d}z^2}u(z)\right]\mathrm{d}z \\ &=\; 2+\frac{1}{\Delta n^2}\int_0^1 u(z)\frac{\mathrm{d}^2}{\mathrm{d}z^2}u(z)\,\mathrm{d}z.\end{aligned} \tag{37}$$

We can write

$$\int_0^1 u(z)\frac{\mathrm{d}^2}{\mathrm{d}z^2}u(z)\,\mathrm{d}z \;=\; u(z)\frac{\mathrm{d}}{\mathrm{d}z}u(z)\bigg|_0^1-\int_0^1\left[\frac{\mathrm{d}}{\mathrm{d}z}u(z)\right]^2\mathrm{d}z. \tag{38}$$

Since our boundary conditions are periodic for $\phi=\pi$, we have

$$u(z)\frac{\mathrm{d}}{\mathrm{d}z}u(z)\bigg|_0^1 \;=\; 0. \tag{39}$$

Since $u^2(z)$ is periodic when $\phi=0$, this condition then holds for both cases of interest.

As a result, we can rewrite the energy expression as

$$\begin{aligned}\langle v_n|\hat{H}|v_n\rangle \;&=\; \Delta E\sum_m m a_m^2 \;+\; \Delta E\int_0^1 z u^2(z)\,\mathrm{d}z \\ &\quad -2g\Delta E\sum_m a_m(a_{m+1}+a_{m-1})\left[1-\frac{1}{2\Delta n^2}\int_0^1\left[\frac{\mathrm{d}}{\mathrm{d}z}u(z)\right]^2\mathrm{d}z\right].\end{aligned} \tag{40}$$

### 4.3. Optimization of the pulse and amplitude

We optimize the pulse by minimizing the energy to obtain

$$\lambda_u u(z) \;=\; z u(z) - g \sum_m a_m (a_{m+1} + a_{m-1}) \frac{1}{\Delta n^2} \frac{\mathrm{d}^2}{\mathrm{d}z^2} u(z) \tag{41}$$

with the boundary condition

$$u(z+1) = -u(z) \quad (\phi = 0), \tag{42}$$

$$u(z+1) = u(z) \quad (\phi = \pi). \tag{43}$$

Optimization of the amplitude leads to the constraint

$$\lambda_a a_m \;=\; -m a_m - g \left[ 1 - \frac{1}{2\Delta n^2} \int_0^1 \left[ \frac{\mathrm{d}}{\mathrm{d}z} u(z) \right]^2 \mathrm{d}z \right] (a_{m+1} + a_{m-1}). \tag{44}$$

Subject to the same boundary conditions as before

$$a_{-m} \;=\; 0 \quad (m = 1, 2, \cdots), \tag{45}$$

$$\lim_{m \to \infty} a_m \;=\; 0. \tag{46}$$

### 4.4. Results

The pulse and amplitudes predicted by this model are very good, similar to those considered in Section 4.3. However, if we calculate the indirect coupling matrix element based on the total energy expression, the results are not particularly satisfactory as illustrated in Fig. 5. At low $g/\Delta n^2$ for this model, the model result appears to diverge from the numerically exact result. The reason for this is that there occur minor differences in the amplitude in this model for $\phi = 0$ and $\phi = \pi$ at low $g$ which has a big impact on the relative total energy. We can eliminate this effect by using instead an estimate based on the pulse eigenvalues

$$\frac{V_{\mathrm{eff}}}{\Delta E} \;=\; \frac{\lambda_u(0) - \lambda_u(\pi)}{4}. \tag{47}$$

The indirect matrix element computed in this way is much better, as can be seen in Fig. 5.

## 5. Continuum Pulse and Continuum Amplitude Model

At larger $\Delta n$, the dimensionless coupling parameter $g$ must be even larger for significant indirect coupling to occur, which results in a much larger number of pulses appearing. To address this, we would like to develop a continuum approximation for the amplitudes.

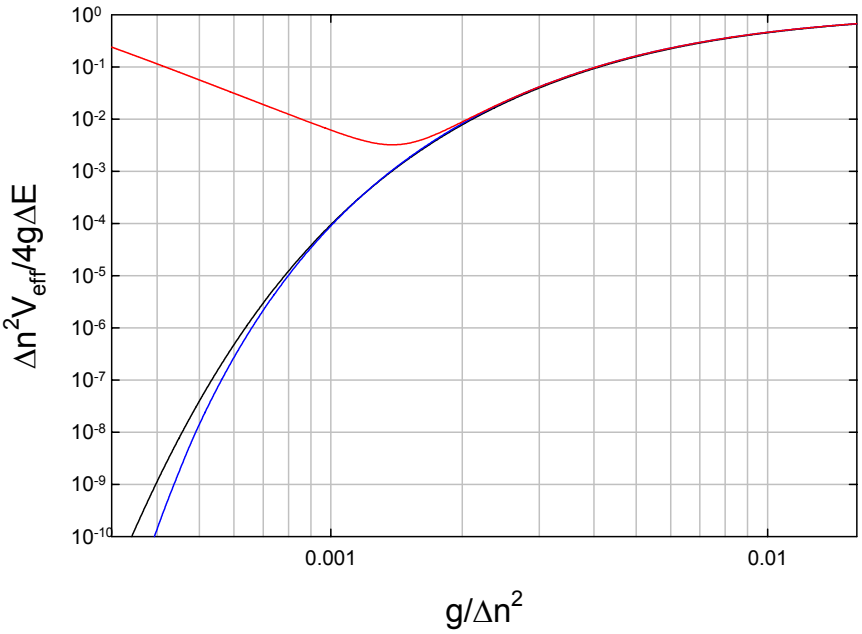


**Figure 5.** Scaled indirect coupling matrix element as a function of $g$ for $\Delta n = 31$; numerically exact result (*black*), scaled matrix element computed from the total energy expression (*red*); scaled matrix element computed from the difference in pulse eigenvalues (*blue*).

### 5.1. Amplitude continuum approximation

We adopt a continuous variable in place of the index $m$

$$m \;\rightarrow\; y \tag{48}$$

and then use a continuous version of the envelope amplitudes

$$a_m \;\rightarrow\; a(y). \tag{49}$$

The energy expression in this model becomes

$$\langle v_n|\hat{H}|v_n\rangle \;=\; \Delta E \int_0^\infty y a^2(y)\,\mathrm{d}y \;+\; \Delta E \int_0^1 z u^2(z)\,\mathrm{d}z$$
$$- 2g\Delta E \int_0^\infty a(y)[a(y+1)+a(y-1)]\,\mathrm{d}y\left[1 - \frac{1}{2\Delta n^2}\int_0^1 \left[\frac{\mathrm{d}}{\mathrm{d}z}u(z)\right]^2 \mathrm{d}z\right], \tag{50}$$

where we assume that

$$\int_0^1 u^2(z)\,\mathrm{d}z \;=\; 1, \tag{51}$$

$$\int_0^\infty a^2(y)\,\mathrm{d}y \;=\; 1. \tag{52}$$

5.2. Large $g$ approximation

We would prefer to work with a differential eigenvalue equation for the optimization of the amplitudes, so we use a Taylor series to approximate

$$a(y+1)+a(y-1) \;=\; 2a(y)+\frac{\mathrm{d}^2}{\mathrm{d}y^2}a(y)+\cdots \tag{53}$$

Once again, if a second-order approximation is good enough, then we may write

$$\int_0^\infty a(y)[a(y+1)+a(y-1)]\,\mathrm{d}y \;=\; 2+\int_0^\infty a(y)\frac{\mathrm{d}^2}{\mathrm{d}y^2}a(y)\,\mathrm{d}y. \tag{54}$$

We can use integration by parts to write

$$\int_0^\infty a(y)\frac{\mathrm{d}^2}{\mathrm{d}y^2}a(y)\,\mathrm{d}y \;=\; a(y)\frac{\mathrm{d}}{\mathrm{d}y}a(y)\bigg|_0^\infty-\int_0^\infty\left[\frac{\mathrm{d}}{\mathrm{d}y}a(y)\right]^2\mathrm{d}y. \tag{55}$$

We expect that the amplitudes decay to zero as $y\to\infty$, but the amplitudes and the first derivative does not vanish at $y=0$; hence

$$\int_0^\infty a(y)\frac{\mathrm{d}^2}{\mathrm{d}y^2}a(y)\,\mathrm{d}y \;=\; -a(0)a'(0)-\int_0^\infty\left[\frac{\mathrm{d}}{\mathrm{d}y}a(y)\right]^2\mathrm{d}y. \tag{56}$$

The energy expression in this approximation becomes

$$\langle v_n|\hat{H}|v_n\rangle \;=\; \Delta E\int_0^\infty ya^2(y)\,\mathrm{d}y \;+\; \Delta E\int_0^1 zu^2(z)\,\mathrm{d}z$$

$$-4g\Delta E\left[1-\frac{a(0)a'(0)}{2}-\frac{1}{2}\int_0^\infty\left[\frac{\mathrm{d}}{\mathrm{d}y}a(y)\right]^2\mathrm{d}y\right]\left[1-\frac{1}{2\Delta n^2}\int_0^1\left[\frac{\mathrm{d}}{\mathrm{d}z}u(z)\right]^2\mathrm{d}z\right]. \tag{57}$$

### 5.3. Optimization of the pulse and amplitudes

We can optimize the pulse $u(z)$ to obtain

$$\lambda_u u(z) \;=\; zu(z) - \frac{2g}{\Delta n^2}\left[1 - \frac{a(0)a'(0)}{2} - \frac{1}{2}\int_0^\infty \left[a'(y)\right]^2\,\mathrm{d}y\right]\frac{\mathrm{d}^2}{\mathrm{d}z^2}u(z) \tag{58}$$

subject to the boundary conditions

$$u(0) \;=\; -u(1) \quad (\phi = 0), \tag{59}$$

$$u(0) \;=\; u(1) \quad (\phi = \pi). \tag{60}$$

The amplitudes are optimized to give the constraint

$$\lambda_a a(y) \;=\; ya(y) - 2g\left[1 - \frac{1}{2\Delta n^2}\int_0^1 [u'(z)]^2\,\mathrm{d}z\right]\frac{\mathrm{d}^2}{\mathrm{d}y^2}a(y) \tag{61}$$

subject to the boundary conditions

$$\lambda_a a(0) \;=\; -2g\left[1 - \frac{1}{2\Delta n^2}\int_0^1 [u'(z)]^2\,\mathrm{d}z\right]\left[a(1) - 2a(0)\right], \tag{62}$$

$$\lim_{y\to\infty} a(y) \;=\; 0. \tag{63}$$

The first of these was selected (as giving the best self-energy) from numerous possible similar boundary conditions based on the ways of estimating the slope at the boundary; this one is adapted from the relation between the discrete amplitude approximation for $a_m$ with $m = 0$. We note that there are relations between the eigenvalue and the factors that appear in these optimization equations, as given in the Appendix.

### 5.4. Airy function solution for the amplitudes

Note that we can solve analytically for the amplitude function in terms of Airy functions

$$a(y) \;=\; C\,\mathrm{Ai}\left(\beta(y - y_0)\right), \tag{64}$$

where $C$ is a normalization constant, and $\beta$ satisfies

$$\frac{1}{\beta^3} \;=\; 2g\left[1 - \frac{1}{2\Delta n^2}\int_0^1 [u'(z)]^2\,\mathrm{d}z\right]. \tag{65}$$

The eigenvalue $\lambda_a$ for this solution is

$$\lambda_a \;=\; y_0. \tag{66}$$

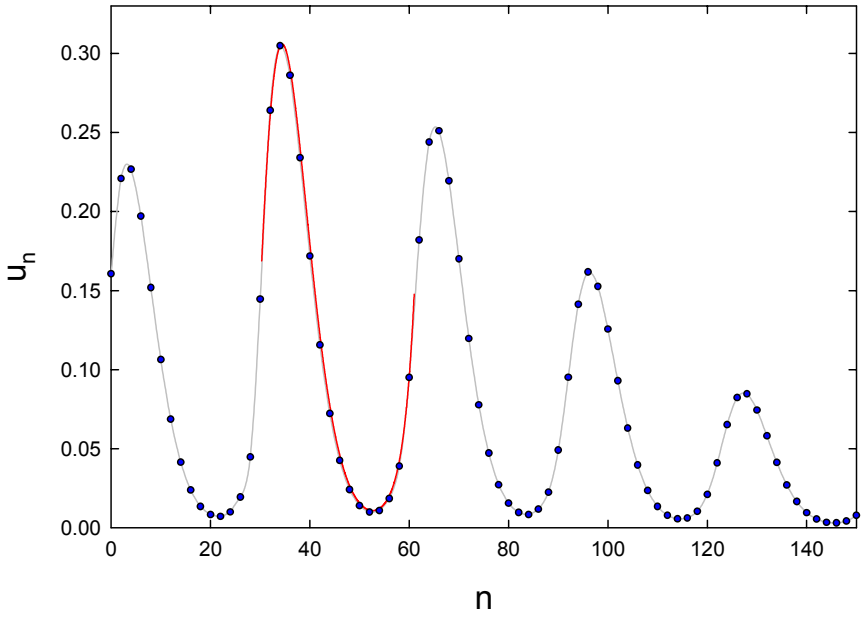


**Figure 6.** Expansion coefficients for $\Delta n = 31$, $g = 2$, and $\phi = \pi$ (*blue points*); optimized product continuum solution for the pulse (*red line*).

The boundary condition at $y = 0$ is satisfied by

$$\lambda_a \mathrm{Ai}\,(-\beta y_0) \;=\; -2g\left[1 - \frac{1}{2\Delta n^2}\int_0^1 [u'(z)]^2\,\mathrm{d}z\right]\left[\mathrm{Ai}\left(\beta(1-y_0)\right) - 2\mathrm{Ai}\,((-\beta y_0)\right], \tag{67}$$

$$\frac{\mathrm{Ai}\left(\beta(1-y_0)\right)}{\mathrm{Ai}\,(-\beta y_0)} \;=\; 2 - \frac{y_0}{2g\left[1 - \frac{1}{2\Delta n^2}\int_0^1 [u'(z)]^2\,\mathrm{d}z\right]}. \tag{68}$$

### 5.5. Evaluation of the continuum pulse and envelope model

Two distinct approximations are made in the continuum model described in the sections above; modeling the pulse as a continuum, and modeling the amplitudes as a continuum. For our test problem with $\Delta n = 31$ and $g = 2$, we find that the pulse (Fig. 6) and amplitudes (Fig. 7) once again are well approximated by the continuum approximation. In general, the continuum approximation seems to be closer for the self-energy than the discrete approximation described previously, as shown in Fig. 8. The indirect matrix element computed from the total energy, and from the pulse eigenvalues, are shown in Fig. 9. One sees that the problem with the total energy expression is now more severe, but the alternate approach of using the pulse eigenvalues seems to give an estimate not too far from the numerically exact result.

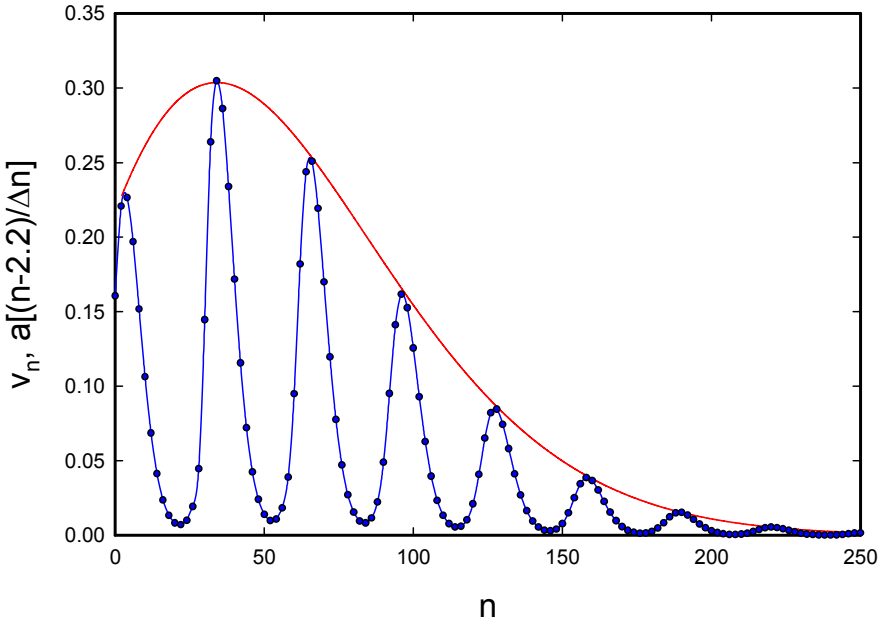


**Figure 7.** Expansion coefficients for $\Delta n = 31$, $g = 2$, and $\phi = \pi$ (*blue points*); optimized product solution for the amplitude (*red line*). We offset the $a(y)$ here to match the peaks of the different pulses (since the first peak does not occur at $n = 0$).

We expect that the pulse and amplitude model comes closer to the exact numerical result when the dimensionless coupling strength is larger, and that the continuum approximation will be better when $\Delta n$ is larger. We can see that this is the case from results for the indirect coupling matrix element shown in Fig. 10.

## 6. Discussion and Conclusions

The lossy spin–boson model is important in our view as the first example of a class of models which demonstrates efficient energy conversion between a two level system and an oscillator when the transition energy $\Delta E$ is a large integer multiple of the oscillator frequency. In spite of the apparent simplicity of the model Hamiltonian, a direct solution of the model when $\Delta n$ is large in the strong coupling regime is not easy. We have developed approximate versions of the model which can be solved much more easily, as described in Section 2

The idea of a pulse and amplitude separation was introduced in earlier work, and it was used to obtain a scaling law in the strong coupling regime. In this paper we revisited the pulse and amplitude model, and developed it much more systematically. This model appears to give good results for both the pulses and amplitudes for the cases studied, as well as for the self-energies. It is in general much more difficult to estimate the indirect coupling matrix element accurately, so that we can get a sense of how good each version of the model is by how well the indirect coupling matrix elements are reproduced.

In the case of the discrete pulse and discrete amplitude approximation, we find the best agreement. When we introduce the continuum approximation for the pulse, we find that estimating the indirect coupling matrix element from

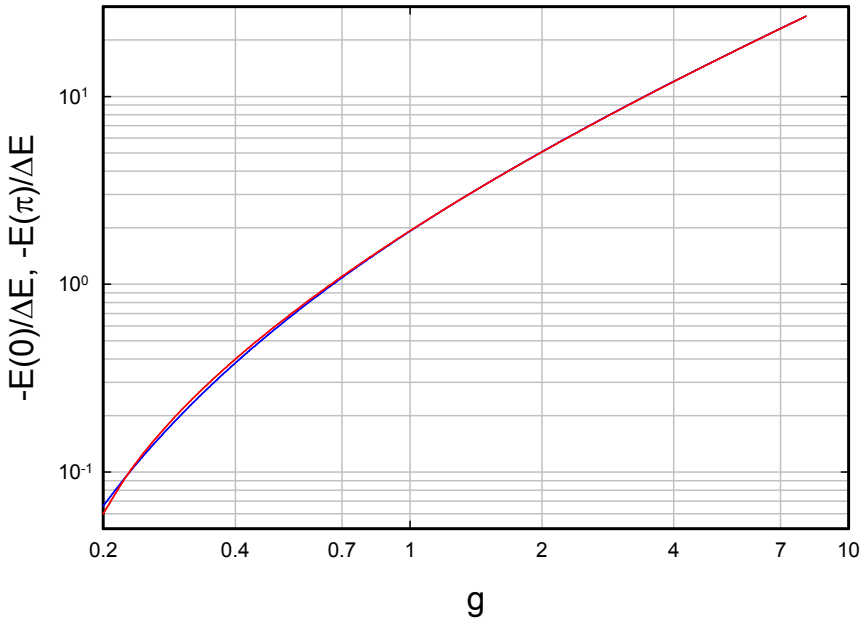


**Figure 8.** Self-energy as a function of $g$ for $\Delta n = 31$; numerically exact results (*blue*), and results computed from optimized pulse and amplitudes (*red*).

the total energy is unreliable in the weak coupling regime. In this case, good results can be recovered if we rely on the difference between the pulse eigenvalues $\lambda_u$ computed for both the $\phi = 0$ and $\phi = \pi$ cases under the assumption that the amplitude is fixed (we chose the $\phi = \pi$ case). In the model where both the pulse and amplitude are continuous, once again the indirect coupling matrix element obtained from the total energy is unreliable in the weak coupling regime, but the results are pretty good if we again use the pulse eigenvalues. If we go back to the discrete pulse and discrete amplitude model and examine the indirect coupling matrix element computed with the pulse eigenvalues, we find that they are very close (the lines overlap on the resulting plots) to those computed with the total energy.

The pulse and amplitude approximation helps to make the lossy two-level model much more understandable. We can see the effect of the amplitudes on the difference in the pulse eigenvalues which approximately determines the splitting. For example, in the strong coupling approximation of Ref. [5], the pulse eigenvalue equation used can be written as

$$\lambda_u u(z) \;=\; zu(z) - \frac{2g}{\Delta n^2}\frac{\mathrm{d}^2}{\mathrm{d}z^2}u(z), \tag{69}$$

while in the pulse and amplitude approximation we may write

$$\lambda_u u(z) \;=\; zu(z) - \frac{2g}{\Delta n^2}\left[1 + \frac{1}{2}\int_0^\infty a(y)a''(y)\,\mathrm{d}y\right]\frac{\mathrm{d}^2}{\mathrm{d}z^2}u(z). \tag{70}$$

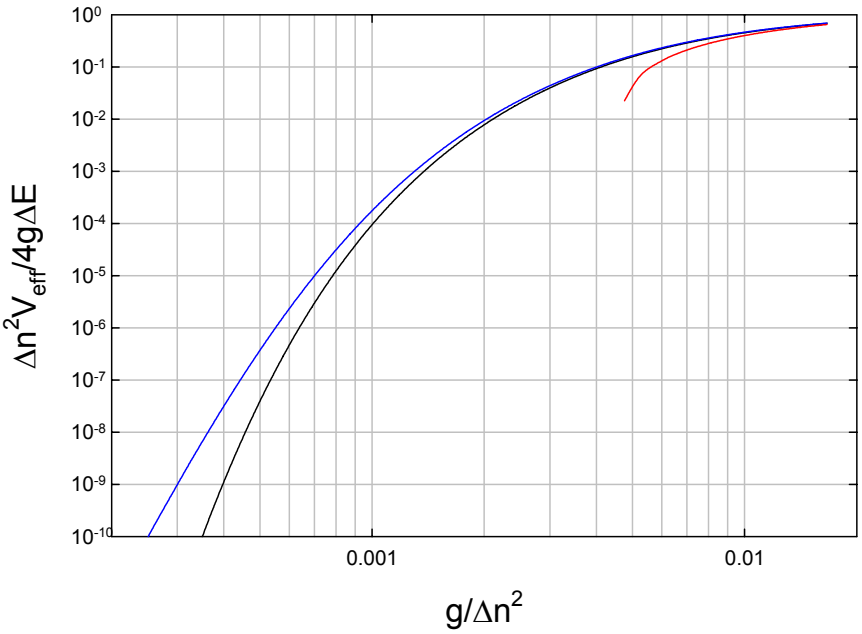


**Figure 9.** Scaled indirect coupling matrix element as a function of $g$ for $\Delta n = 31$; numerically exact result (*black*), scaled matrix element computed from the total energy expression (*red*); scaled matrix element computed from the difference in pulse eigenvalues (*blue*).

Deviations from the strong coupling limit for the pulse come about because the amplitudes are not constant (or linear), and this results in a decrease (since the integral is negative) in the indirect coupling matrix element.

The pulse and amplitude approximation is very powerful, and has applications beyond the lossy spin–boson model. We have found that the approach works well in the case of the generalization of the model to three-level systems.

## Appendix A. Connection between Eigenvalues and Integrals

Once the eigenvalues are found, they can be used to evaluate terms that appear in the energy expression. This is helpful in avoiding the explicit computation of an integral that appears in the other eigenvalue equation, and in the energy expression. We begin by noting

$$\lambda_u \int_0^1 u^2(z)\,\mathrm{d}z \;=\; \int_0^1 z u^2(z)\,\mathrm{d}z - \frac{2g}{\Delta n^2}\left[1 - \frac{a(0)a'(0)}{2} - \frac{1}{2}\int_0^\infty \left[a'(y)\right]^2\,\mathrm{d}y\right]\int_0^1 u(z)\frac{\mathrm{d}^2}{\mathrm{d}z^2}u(z)\,\mathrm{d}z. \tag{A.1}$$

We can rewrite this using the normalization condition as

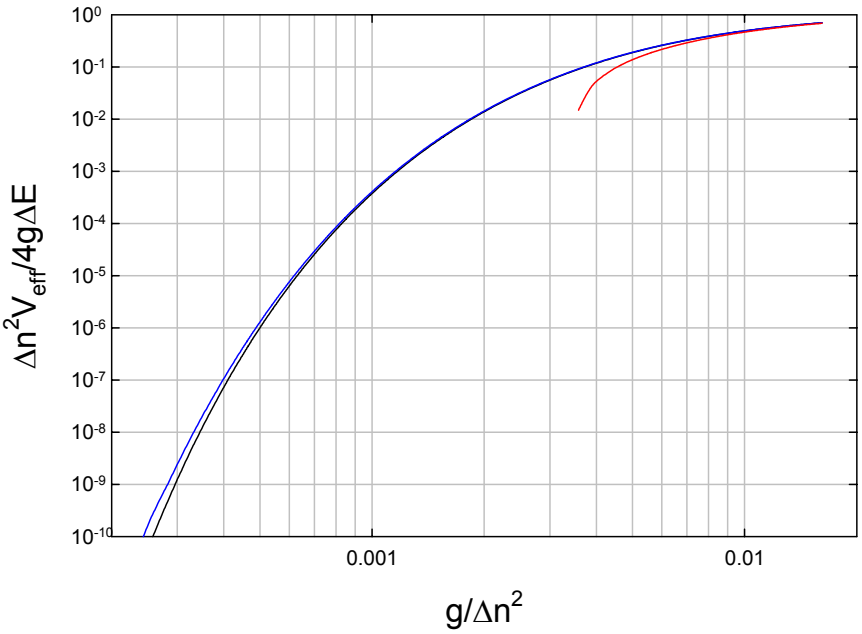


**Figure 10.** Scaled indirect coupling matrix element as a function of $g$ for $\Delta n = 61$; numerically exact result (*black*), scaled matrix element computed from the total energy expression (*red*); scaled matrix element computed from the difference in pulse eigenvalues (*blue*).

$$\frac{1}{2\Delta n^2}\int_0^1 [u'(z)]^2\,\mathrm{d}z \;=\; \frac{1}{4g}\frac{\lambda_u - \displaystyle\int_0^1 z u^2(z)\,\mathrm{d}z}{\left[1 - \dfrac{a(0)a'(0)}{2} - \dfrac{1}{2}\displaystyle\int_0^\infty \left[a'(y)\right]^2\,\mathrm{d}y\right]}. \tag{A.2}$$

Similarly, we may write

$$\lambda_a \int_0^\infty a^2(y)\,\mathrm{d}y \;=\; \int_0^\infty y a^2(y)\,\mathrm{d}y$$
$$- 2g\left[1 - \frac{1}{2\Delta n^2}\int_0^1 [u'(z)]^2\,\mathrm{d}z\right]\int_0^\infty a(y)\frac{\mathrm{d}^2}{\mathrm{d}y^2}a(y)\,\mathrm{d}y, \tag{A.3}$$

$$-2g\left[1 - \frac{1}{2\Delta n^2}\int_0^1 [u'(z)]^2\,\mathrm{d}z\right]\int_0^\infty a(y)\frac{\mathrm{d}^2}{\mathrm{d}y^2}a(y)\,\mathrm{d}y \;=\; \lambda_a - \int_0^\infty y a^2(y)\,\mathrm{d}y, \tag{A.4}$$

$$-\frac{1}{2}\int_0^\infty a(y)\frac{\mathrm{d}^2}{\mathrm{d}y^2}a(y)\,\mathrm{d}y \;=\; \frac{a(0)a'(0)}{2}+\frac{1}{2}\int_0^\infty [a'(y)]^2\,\mathrm{d}y$$

$$= \frac{1}{4g}\frac{\lambda_a-\displaystyle\int_0^\infty ya^2(y)\,\mathrm{d}y}{\left[1-\dfrac{1}{2\Delta n^2}\displaystyle\int_0^1 [u'(z)]^2\,\mathrm{d}z\right]}. \tag{A.5}$$

## References


[1] P.L. Hagelstein and I.U. Chaudhary, Energy exchange in the lossy spin–boson model, *J. Cond. Mat. Nucl. Sci.* **5** (2011) 52.

[2] P.L. Hagelstein and I.U. Chaudhary, Dynamics in the case of coupled degenerate states, *J. Cond. Mat. Nucl. Sci.* **5** (2011) 72.

[3] P.L. Hagelstein and I.U. Chaudhary, Second-order formulation and scaling in the lossy spin–boson model, *J. Cond. Mat. Nucl. Sci.* **5** (2011) 87.

[4] P.L. Hagelstein and I.U. Chaudhary, Local approximation for the lossy spin–boson model, *J. Cond. Mat. Nucl. Sci.* **5** (2011) 102.

[5] P.L. Hagelstein and I.U. Chaudhary, Coherent energy exchange in the strong coupling limit of the lossy spin–boson model, *J. Cond. Mat. Nucl. Sci.* **5** (2011) 116.

[6] M. Fleischmann, S. Pons and M. Hawkins, *J. Electroanal. Chem.* **261** (1989) 301; errata **263** (1990) 187.

[7] M. Fleischmann, S. Pons, M.W. Anderson, L.J. Li and M. Hawkins, *J. Electroanal. Chem.* **287** (1990) 293.